Superconductor ceramics behavior analyses during service by speckle metrology

S Recuero, N Andrés, M P Arroyo, F Lera*, L A Angurel*
Instituto de Investigación en Ingeniería de Aragón (I3A), Universidad de Zaragoza
Facultad de Ciencias, c/ Pedro Cerbuna 12, 50009 Zaragoza, Spain.
*Instituto de Ciencia de Materiales de Aragón (C.S.I.C.-Universidad de Zaragoza),
c/ María de Luna 3, 50018 Zaragoza, Spain.

ABSTRACT

This paper shows the feasibility of applying speckle techniques as a non-destructive evaluation of the performance of ceramic high temperature superconducting materials. Firstly, Digital Speckle Pattern Interferometry has been applied to test these materials during service, with the sample cooled to liquid nitrogen temperatures, to detect where a hot spot will be generated. Surface degradation due to humidity has also been studied. Speckle Photography, whose optical setup is simpler, has been selected for this study.

Keywords: Speckle, DSPI, inhomogeneous heating detection, DSP, environmental degradation

1. INTRODUCTION

One of the main technological problems of ceramic high temperature superconductors is inhomogeneous heating due to hot spot generation [1]. Due to the low thermal conductivity of these materials, the heat dissipated at the points where the superconducting properties are the poorest, produces local heating. As this heating makes the superconductor to behave worse, the heating increases at a high rate, deteriorating the sample properties in a short time and eventually reaching the melting point. In order to improve the development of technological applications with these materials it is convenient to know the origin of these hot spots. Until now, the typical characterization of superconducting ceramics based on usual electrical transport measurements only gives information integrated along the length on the sample. The beginning of the quench can also be measured by recording the bubble formation on samples immersed in liquid nitrogen [2], but a high current passing through the material is usually required to detect the hot spot generation. A non-destructive technique that could detect where a hot spot will appear before excessive heat is generated would be greatly desirable.

In this sense, optical measurement techniques are becoming valuable tools due to their non-destructive nature. Digital Speckle Pattern Interferometry (DSPI) is a well-established technique to measure small displacements of diffusely reflecting objects [3]. This technique produces fringe patterns by comparing two different specklegrams and has some interesting properties such as, non-contact nature, digital recording, high sensitivity and full-field analysis. This technique has already been tested in a high temperature superconductor during service demonstrating the possibilities of the technique for hot spot detection [4], without changing the sample properties because only a small current is required. These studies are important because once the hot spot is located, microstructural analysis can be performed in order to correlate this position with the appearance of a given microstructural defect on the sample.

Environmental surface degradation is another of the greatest problems in the design of durable products because some chemical phases present in these materials react with humid air [5]. The stability of these materials has been tested in different environments, like water, moisture and several organic solvents. There is a demand for optical measurement of degradation due to their local resolution. As the microscopic information is transferred to the speckle, if the surface undergoes any micro-alterations a related change in the scattered light field is observed. What it is really interesting is to detect the origin of the degradation process in its early stage and to investigate the areas where the degradation begins

with the idea of designing more effective protection system. Speckle Photography has been selected as the most adequate technique because its symply setup [6] and its ability to produce both a global parameter and a full field information.

2. DIGITAL SPECKLE PATTERN INTERFEROMETRY

In DSPI the interference between an object wave and a reference wave is recorded [7]. In solids mechanics, the object wave is formed by the light scattered by the solid surface after being illuminated by an extended laser beam and focused onto a CCD detector using a convergent lens. The reference beam, obtained by diverting a small amount of the main laser beam, is divergent with the focus at the same distance from the sensor as the camera lens aperture. Both beams are made to overlap by means of a cube beam-splitter placed in front of the CCD sensor, as it is shown in Figure 1. The interference pattern is known as specklegram because of its speckled appearance.

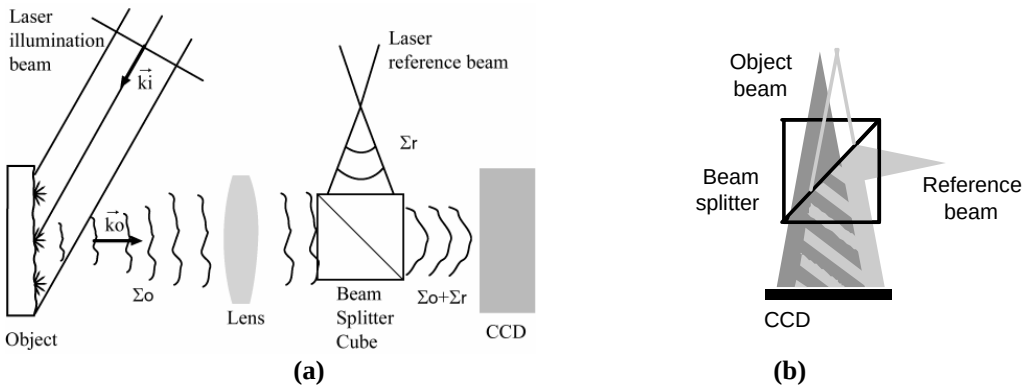

Fig. 1. (a) Optical setup of SPS-DSPI technique, **(b)** reference and object wave overlapping.

A conventional DSPI set-up can be turned into a SPS-DSPI setup by shifting the origin of the smooth divergent reference wave with respect to the lens centre by a certain amount Δx. This generates a linear phase shift in the x-direction of the image. As the phase-shifted data are recorded simultaneously on adjacent pixels, the speckle size must be increased up to about three pixels. In order for the sensor to resolve the modulation frequency, a maximum phase shift of 2π over three pixels has to occur [8].

The phase recorded at each position is a spatially random magnitude because the object is a speckle field. However, for each (x,y) position the change in ϕ_o, $\Delta\phi_o$, is not random but related to the local displacement. This relationship can be expressed as

$$\Delta\phi_o = \vec{K}\cdot\vec{L} \qquad (1)$$

where $\vec{L}$ is the local displacement, and $\vec{K} = \vec{k}_o - \vec{k}_i$ is the sensitivity vector, being $\vec{k}_o$ and $\vec{k}_i$ vectors in the observation and the illumination directions respectively with modulus $2\pi/\lambda$, and λ being the laser wavelength in the fluid.

The most appropriate method for analysing the SPS-specklegram is a global and frequency based method called Fourier transform method (FTM) [9]. The principles of this method are shown in Fig. 2. It shows a typical speckle pattern with carrier fringes (fig. 2a) and its Fourier transform (fig. 2b) in which three terms can distinguish. The speckle halo is in the middle while the two lobes, that come from the interference effects, are shifted symmetrically from the centre by an amount that depends on the introduced carrier frequency. Only one lobe is selected and its inverse Fourier transform is calculated to obtain the phase map.

During the measuring process series of images are recorded. The phase difference map is obtained by subtracting the object phase maps corresponding to two specklegrams. Let us remark that the phase difference is calculated with respect to some initial reference situation, which in general corresponds to the undeformed state. The calculated phase difference values lie in the range of 2π and values outside this range are wrapped. In this type of wrapped phase maps null phase is mapped into black, while 2π is mapped into white. An unwrapping process, in which the phase is extended to a continuous range of more than 2π, is required for determining the deformation.

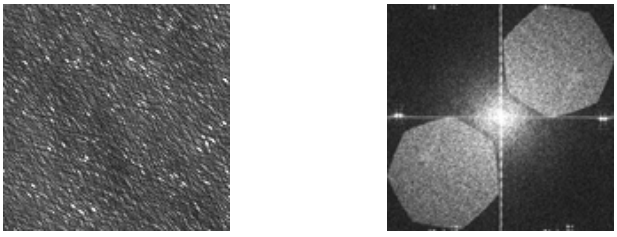

(a) **(b)**

Fig. 2. (a) 128x128 region of a typical specklegram obtained with SPS modulation. **(b)** Its Fourier Transform

3. EXPERIMENTAL SETUP

SPS-DSPI has been implemented for measuring on ceramic superconducting materials during service as shown in Fig 3a. The sample is illuminated by a collimated laser beam from a 17 mW He-Ne laser. Illumination and observation directions are perpendicular to each other and both at an angle of 45º with the object surface. Images are recorded with a digital CCD camera (652x494 pixels, 7,4 μm /pixel and 256 grey levels) using a 120 mm focal length lens. An aperture of f/16 and a magnification of 0.28 are used for the recording. With these experimental conditions, the recorded object area is 23.9x13 mm^2. As the height of the samples is smaller than its length, the magnification has been chosen to cover a significant part of the CCD sensor height. For achieving the spatial phase shifting, the origin of the reference wave, located at the same distance from the sensor as the camera lens aperture, is transversally displaced by about 3 mm in each direction. For this purpose the 20x microscope objective is placed on a micrometric movement stage. With this setup, the phase difference $\Delta\phi$ gives information mainly on the out-of-plane displacement; the sensitivity of the technique has been determined to be 0.45 μm per fringe.

As the operating temperature for this kind of ceramic superconductors is below 90 K, the sample must be cooled down with liquid nitrogen. A glass dewar, with a 85 mm high window along its perimeter, has been designed. In our experiments, optical access is only needed for the illumination and observation of the sample. Thus, only two windows at 90º have been left without covering. Each window has been heated with an external manganine resistance to avoid condensation in the external wall. Since phase variations are much smaller in gaseous media than in liquid media the sample should be cooled down by conduction instead by direct immersion in liquid nitrogen [4]. Thus, the sample has been thermally fixed to a big aluminium plate with its lower part immersed in liquid nitrogen, whose level is kept just below the sample (fig. 3b). The left end of the sample is fixed by a screw to avoid bulk movements. The current is applied by means of two silver current contacts and the electrical wires come from the top but are immersed in the nitrogen before contacting the superconductor to minimize the amount of transferred heat. Another couple of wires are attached to the sample for measuring the voltage drop between them, ΔV, that gives information on the resistance. A piece of paper is placed between the sample and the plate in order to keep the electrical insulation. The thermal contact has been improved by using a layer of APIEZON® N grease. After making rotary pump vacuum (~10^{-1}Atm) inside the dewar, undesired phase variations are minimized and the sample can be studied for at least half an hour.

Let us note that, although some discontinuity in the phase difference map might be observed in the borders of the sample, it is difficult to precisely determine the position of the sample in the map. This problem has been overcome by taking a sample photograph in each experiment. The sample limits in the phase difference maps will be obtained from the corresponding photographs.

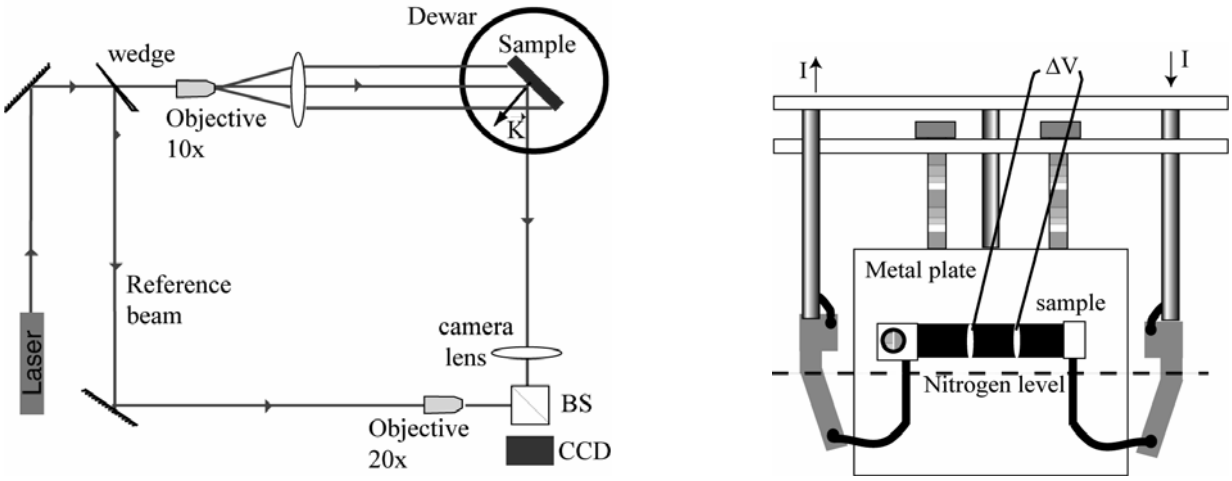

(a) **(b)**

Fig. 3. (a) Optical setup for DSPI **(b)** sample holder

4. HOT SPOT GENERATION ON CERAMIC SUPERCONDUCTORS

DSPI has been tested on textured $Bi_2Sr_2CaCu_2O_{8+\delta}$ (Bi-2212) high temperature superconducting bulk samples. The samples were textured using a Laser Zone Melting (LZM) technique [8]. A continuous diode laser beam is focused on the sample surface along a transverse thin high power line. The laser induces a molten zone that is moved along the sample. This process induces a texture in the superconducting grains. Both surfaces of the sample have been textured in order to avoid the bending of the superconducting ceramic during the annealing [9] due to the differences in density between the polycrystalline precursor and the textured material. The samples show some anisotropy in their texture and superconducting properties. For simplifying the current set up and minimizing the heat generated at the electrical contacts, DSPI has been tested in samples whose critical intensity at 77 K, $I_C(77K)$ is lower than 15 Amperes. In addition, the voltage generated at the centre of the sample (distance between contacts around 10 mm) is recorded during experiments. The results that are presented in this work correspond to two samples with a length of 40 mm, a width of 7 mm and a thickness of 1.4 mm. In case of sample A, the critical current value at 77 K is 5 A and at room temperature, the sample has a resistance of 27.95 mΩ. In case of sample B a transverse defect has been induced on the sample with a mechanical incision. The critical current at 77 K in the region without defect is 50 A; close to the incision, this value is reduced to 15 A and the room temperature resistance value is 9.4 mΩ.

Series of specklegrams at 400 ms intervals with 2 ms exposure times were recorded. The initial experiments have been performed at room temperature (non superconducting state). In these conditions, the sample resistance is proportional to the temperature and, in consequence, the variation of resistance can be considered as a measure of the temperature changes induced in the sample due to the Joule heating generated by the current. The evolution of the fringe pattern with time for a fixed current of 2 A is presented in Figure 4 a-d. The pattern shows a set of parallel fringes whose number increases with time until a final stationary state is reached. A similar behaviour is observed with I=2.5 A (Fig. 4 e-h). In this case the stationary state is reached with 8 fringes, a higher number than in the case of I=2 A due to the higher heating induced by the current.

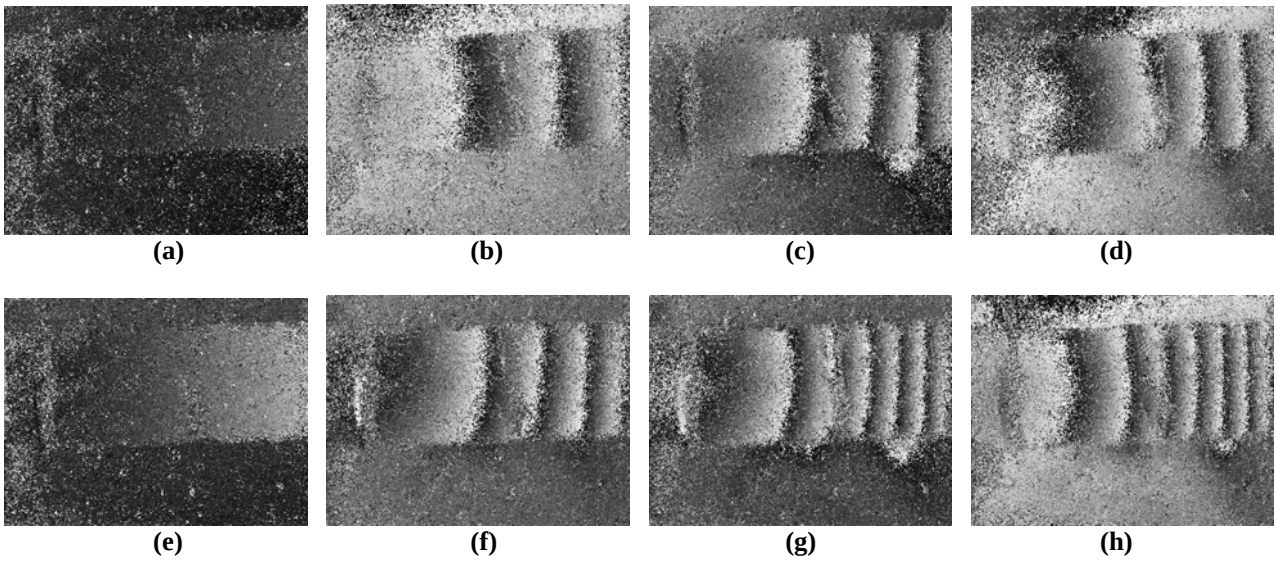

Fig. 4. Fringe pattern is sample A at room temperature: **(a)** I=2 A, t=10s, **(b)** I=2 A, t=20s, **(c)** I=2 A, t=40s, **(d)** I=2 A, t=80s, **(e)** I=2.5 A, t=10s, **(f)** I=.52 A, t=20s, **(g)** I=2.5 A, t=40s, **(h)** I=2.5 A, t=80s.

The evolution of these fringe patterns is very similar to the variations observed in the time evolution of the room temperature resistance. During this time the resistance of the sample is increasing (Fig. 5), which means that the sample is warming up and the evolution is similar to those obtained in the DSPI experiments. After some time, the system reaches stationary conditions and the temperature becomes constant. All these observations suggest that the main contribution to the fringe pattern comes from dilatation. This is more evident observing the data presented in Figure 6. In this figure, the fringe pattern has been obtained comparing two images recorded at two instants in which the difference in resistance is the same, in particular, 0.17 mΩ. The first pattern has been obtained with a current of 2 A and comparing the images in the instant t=10.8 s and t=70.0 s. In the second case, the images correspond to I=2.5 A, and the instants are t=14,4 s and t=68 s.

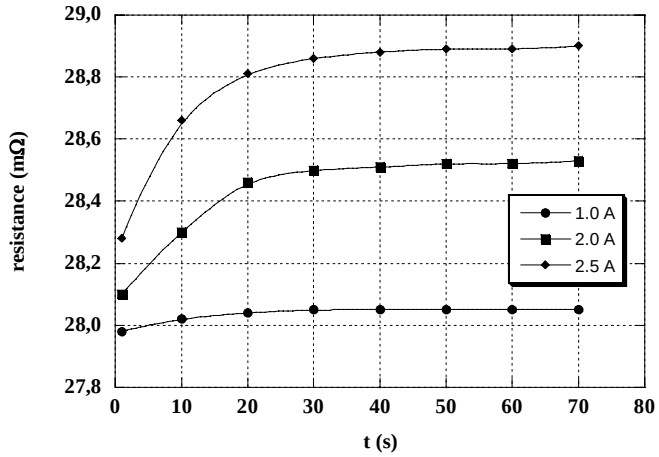

Fig. 5. Temporal evolution of the room temperature resistance in sample A with time for different currents.

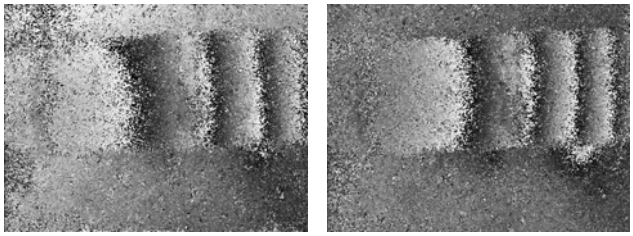

(a) **(b)**

Fig. 6. Fringe pattern obtained by comparing two images with the same ΔR=0.17 mΩ. **(a)** I=2 A, images recorded at 10.8 s and 70 s, **(b)** I=2.5 A, images recorded at 14.4 s and 68 s.

Due to the configuration of the experiment, the rear surface, in contact with the metal plate, has a lower temperature than the front surface. This difference in temperatures produces a bending. This material bending is the main contribution to this pattern of parallel fringes. In these experiments, the sample perfectly recovers its undeformed state shortly after switching off the current.

At cryogenic temperatures, the obtained fringe pattern is completely different. If the current applied is bigger than I_C, the point with poorest superconducting properties starts to dissipate. Thus, a local temperature increase is produced and the adjacent points can reach the non-superconducting state starting dissipation too. The heat propagation rate is very low due to the very low thermal conductivity values of the material and the resistance of the sample increases at a high rate. In the case of sample B, the fringe pattern is determined by the mechanical incision that has been done on the sample surface (Fig. 7a). At a temperature in which the critical current value is 2 A and the applied current is 15 A, in the initial stage, a clear circular pattern can be observed, whose origin is located close to the defect (Fig. 7 b-d). The resistance of the sample in this experiment presents a sharp increase that starts at t=30 s. The optical technique is able to detect this defect before; the fringe pattern shows at 20 s the presence of the hot spot and its localization. The defect has to be determined in its early stage because the evolution of the heating reaches all the sample hiding the origin of this hot spot, as can be observed in the image recorded after 50 s.

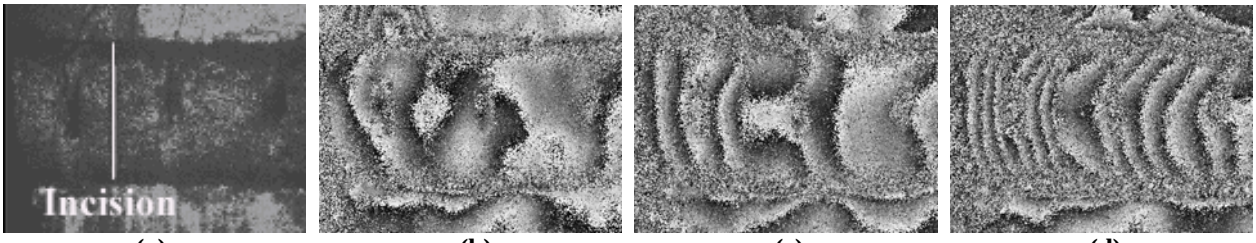

(a) **(b)** **(c)** **(d)**

Fig. 7. (a) Aspect of sample B showing the mechanical incision. The fringe patterns have been obtained at a temperature in which I_C=2A and the applied current is 15 A after **(b**) 21 s, **(c)** 30 s and **(d)** 50 s.

The aim of this work is to determine if this technique is adequate to detect internal defects on a superconducting sample that can be responsible of the hot spot generation. The same kind of experiments have been performed on sample A at temperatures between 77 K and 90 K, with applied currents that are three times higher than the critical current values at a given temperatures. Figure 8 a-c shows the temporal evolution of the fringe pattern when I_C=5A and the applied current was 15 A. Clearly the fringes have their origin in a point of the sample. It has been calculated that the temperature change required to detect the defect is about 100 K. These temperature changes do not deteriorate the sample properties and the sample can be tested several times. Once the position of the defect has been determined, other experiments have been performed with currents up to 100 A over 500 ms. In this case, the heat generated in this point induces a local temperature increase that can reach the melting point. During this experiment the sample melted. Figure 8d show how the fracture surface look like. This point coincides with the prediction of the DSPI experiments.

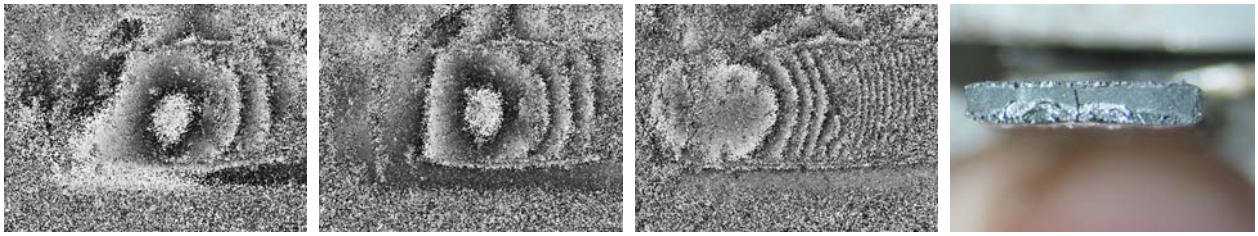

(a) **(b)** **(c)** **(d)**

Fig. 8. Fringe patterns observed in sample A in the superconducting state with I=15 A when I_C=5 A. **(a)** Pattern after 24.4 s, **(b)** after 24.8 s and **(c)** after 40 s. **(d)** Fracture surface after a destructive experiment.

5. SPECKLE PHOTOGRAPHY

In Digital Speckle Photography (DSP) focused images of the object surface are recorded with a CCD camera. The surface under investigation is illuminated by a collimated beam of coherent light at an angle θ (Fig. 9). Since the microscopic properties of the surface are transferred to the speckle pattern in the image, the surface changes can be inferred from a comparison of the speckle patterns obtained from different states of the object [6]. The similarity of two speckle intensities is difficult to estimate directly because of their random character. The required task is to obtain a quantitative measure for the similarity of speckle patterns and to relate its change to corresponding changes in the surface properties. The best way to measure the similarity of two speckle patterns is by calculating its correlation coefficient:

$$c_{12} = \frac{\langle I_1 I_2 \rangle - \langle I_1 \rangle \langle I_1 \rangle}{\left[\left(\langle I_1^2 \rangle - \langle I_1 \rangle^2 \right) \left(\langle I_2^2 \rangle - \langle I_2 \rangle^2 \right) \right]^{1/2}} \qquad (2)$$

where I_1 and I_2 are the intensities at each recorded image and the angle brackets denote the spatial average in the image. However, C_{12} is not only affected by microstructural changes but also by surface displacements. These displacements can be taken into account by calculating the normalized 2-D cross correlation function, where the correlation coefficient as a measurement of speckle similarity can be inferred from the shape and height of the main correlation peak. When the surface displacement is on its plane, the correlate coefficient is given by the maximum value. The position of the correlation peak is a measurement of the in plane surface displacement, which is the typical application of DSP. In this case, the correlation function is calculated in several sub-regions of the image allowing to obtain the in plane displacement field for the whole surface. In the same way, a 2-D map of correlation coefficients can be obtained by calculating this coefficient in several sub-regions of the image. This procedure should allow determining the areas where the surface degradation starts.

The DSP optical set up is shown in figure 9. The sample is illuminated with a collimated laser beam at an angle of 30º and imaged onto a CCD camera by a 120 mm focal length lens with a magnification of 0.5. The CCD sensor has 1280x1024 pixels with a size of 6.7 μm/pixel. The images have 4096 grey levels. The sample was placed perpendicular so that surface is on focus. An 80 mW solid state laser have been used as the coherent illumination source.

The samples are placed in a glass vase filled with water to accelerate the degradation process. The object surface is located close to the vase front wall to reduce the influence of the water refraction index change in the speckle pattern structure.

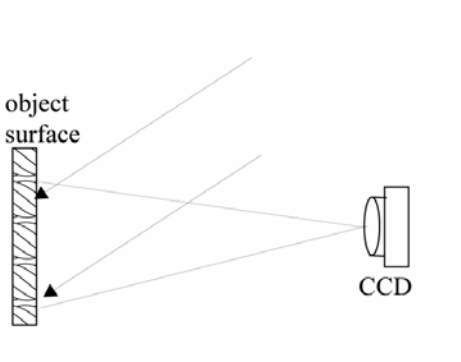

Fig. 9: Set-up for Speckle photography

Series of images are sequentially recorded while the degradation is taking place. Each image can be compared with the image in the initial state in order to obtain the time development of the degradation. However, since all the maps are stored in the computer, it is also possible to compare any two states of the process to obtain additional information.

6. ENVIRONMENTAL DEGRADATION

This technique has been applied to samples with the same characteristics that sample A at room temperature, and with one part of the sample immersed in water (Fig. 10). In the first experiments, the evolution of the correlation coefficient as a global measurement has been studied. The correlation coefficient corresponding to a big area (280 x 280 pixels) has been calculated. The image taken from the sample corresponds not only to the part that is immersed in water but they also include a portion of the sample which is in ambient air. This part of the sample is used as a reference in order to check if they are other processes apart from the water induced degradation, which affect the correlation coefficient. Figure 11 shows the correlation coefficient obtained from both, the region in air and the region in water, from images taken for more than one hour. In air, the coefficient decreases slowly and continuously down to a value of 0.7. In water, the loss of correlation is bigger and changes at the beginning are more significantly decreasing to values lower than 0.5 in less than 30 seconds (Fig. 11 b).

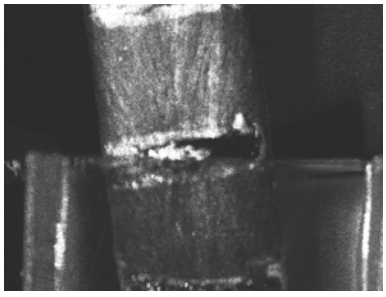

Fig. 10: Experimental arrangement with part of the sample immersed in water.

A quantitative interpretation of the speckle correlation coefficient in terms of changes at the surface it a very hard task. The aim of our work is to know where the degradation process starts. Thus, a posterior micro structural analysis of the area can be performed in order to know which are the weaker regions in the sample. This study requires local analysis with window sampling. The correlation coefficient has been calculated with windows of 16x16 pixels, and a 2-D correlation coefficient map is plotted with black corresponding to high correlation (undisturbed areas) and white to low correlation (highly deteriorated areas). The region in air (fig. 12) shows a high coefficient correlation that indicates no

changes are taken place. Only after a very long time some changes will be observed due to humidity. In the area immersed in water, the degradation starts in the edges of the sample and it is already observed after only 1 s.

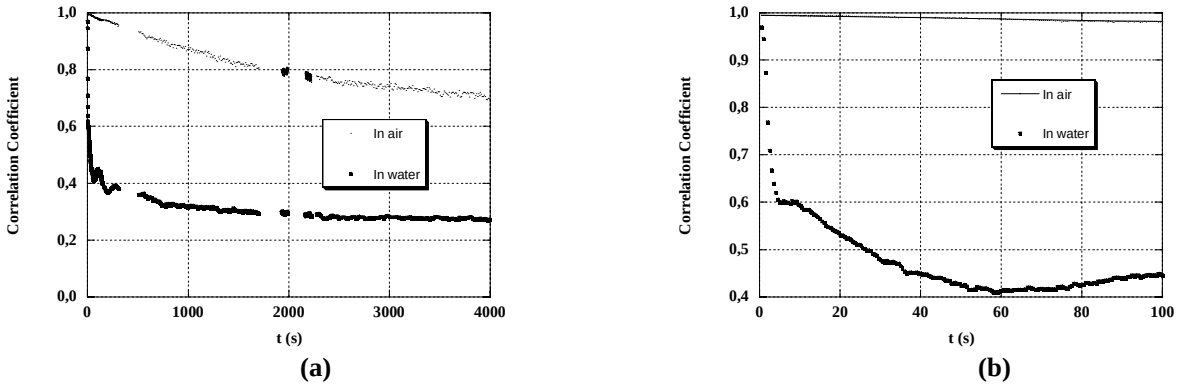

Fig. 11 Correlation coefficient versus time for the sample in air and in water. **(a)** for the whole time history **(b)** for the first 100 s.

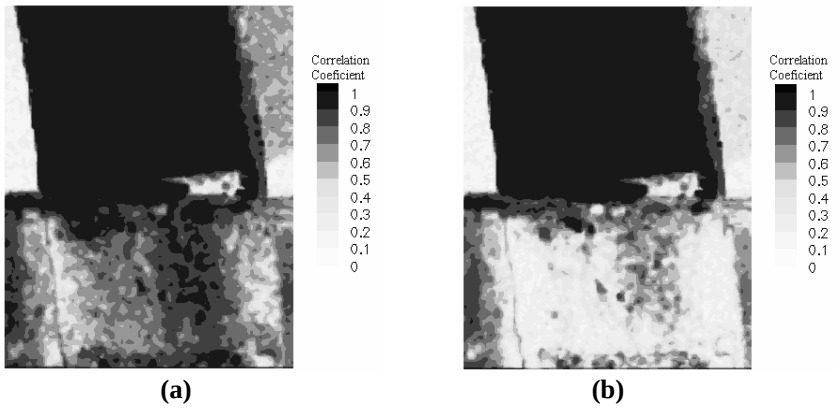

Fig. 12: (a) Correlation map after 1 s and **(b)** after 2.5 s.

The degradation process has also been analysed on a superconducting Bi-2212 thick film deposited on a monocrystalline MgO substrate [12]. Typical dimensions of the samples used in this study are 5 cm x 1 cm. Using laser machining, a meander configuration has been induced on the sample in order to increase the superconducting current path length and, in consequence, the sample resistance. This is required in some high power applications, like fault current limitation. Due to the machining lines, there are non laser textured regions inside the sample that can be affected by to the ambient humidity more strongly than the laser textured regions.

The full field analysis, using sampling windows, gives information about the areas in which the process starts (Fig. 13 a-c). The narrow white lines observed after 10 seconds are increasing wider and wider. As was expected, the degradation starts in the areas in which the high density superficial layer, induced in the texturing process, is destroyed by the laser machining during the fabrication of the meander.

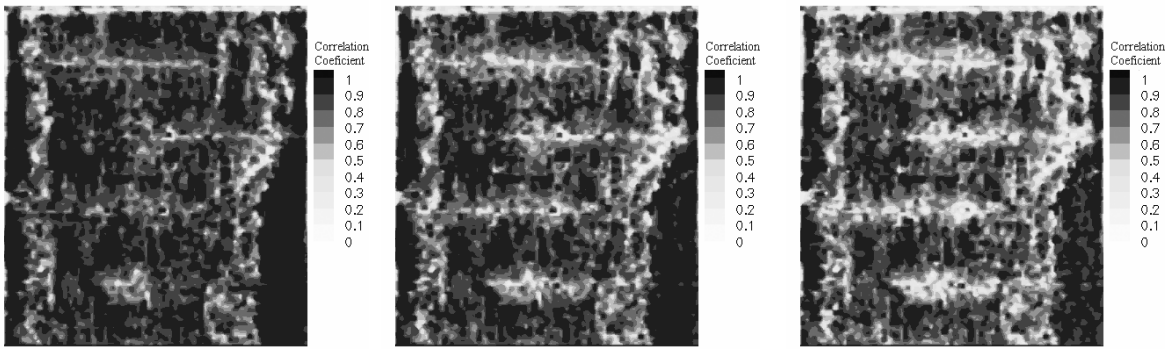

Fig. 13. Correlation map after **(a)** 10s, **(b)** 10 min, **(c)** 60 min

7. CONCLUSIONS

Digital Speckle Pattern Interferometry has been applied in superconducting ceramics to detect the localization of inhomogeneous heating. The changes in resistance are related to the fringe pattern. Experiments were performed at room temperature and at temperatures close to 77K. In the first case a set of parallel fringes are obtained, whose number is related to the temperature changes induced by Joule heating. In the second case, the hot spot localization is determined in the initial stages. The produced heating levels are low enough to avoid any degradation of the superconducting properties of the material.

Digital Speckle Photography has been demonstrated as a adequate technique to detect environmental degradation process in their initial stages.

With both techniques, the aim is the detection of areas of interest for a posterior microstructural analysis in order to determine which are the defects in the microstructure of these material that are relevant in the hot spot generation and in the environmental degradation.

ACKNOWLEDGMENTS

This research was supported by the Spanish Ministerio de Ciencia y Tecnología (MAT2002-04121-C03-01 and -02) and by the Diputación General de Aragón (G.I.C., Optical Holography and Metrology and Applied Superconductivity groups).

REFERENCES

1. M. Noe, K.P. Juengst, F.N. Werfel, S. Elschner, J. Bock, F. Breuer, R. Kreutz, "Testing bulk HTS modules for resistive superconducting fault current limiters", IEEE Transaction on applied superconductivity **13**, 11976-1979 (2003).
2. K B Park, J S Kang, B W Lee I S Oh, H S Choi, H R Kim, O B Hyun, "Quench behavior of YBaCuO films for fault current limiters under magnetic field", IEEE Transaction on applied superconductivity **13**, 2092-95 (2003).
3. P.K. Rastogi, editor. Digital Speckle-Pattern Interferometry and related techniques, Wiley (2001).
4. S Recuero, N Andrés, J Lobera, M P Arroyo, L A Angurel, F Lera, "Application of DSPI to detect inhomogeneous heating on superconducting ceramics" Meas. Sci. Technol, 16, 1030-1036 (2005)
5. D. Lee, R.A: Condrate Sr., J.A. Taylor, "The environmental degradation mechanism and protective organic thin film coatings on s high-temperature bismuth-cuprate superconductor", Physica C 350, 1-16 (2001)
6. K.D. Hinsch, T. Fricke-Begemann, G. Gülker, K. Wolff, "Speckle correlation for the analysis of random processes at rough surfaces. Optics and Lasers in Engineering, 33, 87-105 (2000).

7. K. Creath, in D.W. Robinson, G.T. Reid (Eds.) Interferogram Analysis, Institute of Physics Publishing, Bristol, 1993, p 94.
8. K. Creath, "Phase-shifting speckle interferometry", App. Opt., **24**, 18, 3053-3058, 1985.
9. M. Takeda, H. Ina, S. Kobayashi, "Fourier-transform method of fringe-pattern analysis for computer based topography and Interferometry", J. Opt Soc. Am. 72, 156-160 (1982)
10. M. Mora, J.C. Díez, C. I. López-Gascón, E. Martínez, G.F. de la Fuente, "Laser textured Bi-2212 in planar geometries", IEEE Trans. Appl. Supercond. 13 3188-3191 (2003)
11. M. Mora, C. López-Gascón, L.A. Angurel, G.F. de la Fuente, "The influence of support temperature on Bi-2212 monoliths textured by diode laser zone melting", Supercond. Sci. Technol. 17, 1329-1334 (2004)
12. M. Mora, F. Gimeno, L.A. Angurel, G.F. de la Fuente, "Laser zone melted $Bi_2Sr_2Ca_2Cu_2O_{8+\delta}$ thick films on (100) MgO substrate", Supercond. Sci. Technol. 17, 1133-1138 (2004)